

Contributions of two-gluon exchange diagrams to the NN spin-orbit interaction

Yiharn Tzeng*

*National Research Institute for Mathematical Sciences, Council for Scientific and Industrial Research,
Pretoria 0001, Republic of South Africa*

and Institute of Physics, Academia Sinica, Nankang Taipei, Taiwan 11529, Republic of China

(Received 23 December 1986)

Contributions of the two-gluon exchange diagrams to the nucleon-nucleon spin-orbit interaction are investigated via the Glauber approximation, and comparisons are made with the gluon-quark exchange diagrams calculated in the resonating group method. Numerical results at $E_{\text{lab}} = 800$ MeV show that contributions from these diagrams are relatively small as compared to those from the resonating group calculations when the oscillator parameter λ of the three-quark cluster and the interaction range a are fitted from the nucleon radius r_N at 0.83 and 0.59 fm. A non-negligible contribution for λ and a at $r_N = 0.42$ fm. Possible reasons are briefly discussed.

I. INTRODUCTION

The understanding of the nucleon-nucleon (NN) interaction has for a very long time been a fundamental problem in nuclear physics. Although the characteristics of NN medium- and long-range interactions can be well described by meson exchange potentials, the short-range part of the interaction is still not well understood. Unfortunately, many important aspects of physics originate from the short-range behavior of the NN force.

Because nucleons are made up of quarks, it is quite natural to expect that quarks may play an important role in the short-range NN interaction. Extensive investigations have been made of the NN short-range repulsion and the spin-orbit interaction through quark models. The spin-orbit interaction, particularly through its spin dependence, may enable us to extract some valuable information on the NN short-range force.

Much theoretical effort^{1,2} has been devoted to studying the NN spin-orbit force via quark models. Most of these studies used the nonrelativistic resonating group method³ (RGM) as their framework. In these calculations, the nucleon is treated as a three-quark color singlet cluster, with the quarks in the lowest $(1s)^3$ state. The wave function of the NN system is antisymmetrized in such a way that quarks are allowed to interchange between different clusters. Because the nucleon is a color singlet, the direct one-gluon exchange interaction [Fig. 1(a)] vanishes. Hence the lowest-order diagrams calculated in the RGM are those of quark-gluon exchanges, as shown in Figs. 1(b) and 1(c). Although the elementary quark-quark spin-orbit force is not isospin dependent, the NN interactions derived from the exchange of quarks are isospin dependent.

However, the question arises whether the diagrams calculated in the RGM are really the lowest order ones. At first, it is not clear whether the two-gluon exchange diagrams, as shown in Fig. 2, can be ignored when compared to those calculated in the RGM. It is thus desirable to investigate the importance of the two-gluon exchange diagrams. This is the purpose of this paper.

The framework used in this work is the Glauber approximation,⁴ which has been used successfully to explain medium and high energy nucleus-nucleus scattering problems. For the sake of convenience, the form and parameters used for the quark-quark spin-orbit potential are exactly the same as those in Ref. 2, where the t -matrix elements of the NN spin-orbit interaction were calculated via

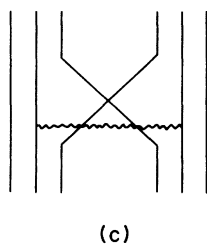
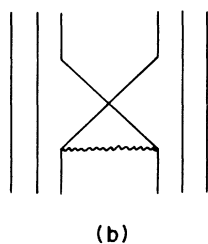
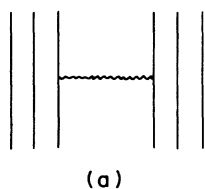


FIG. 1. (a) The direct one-gluon exchange diagram, which gives no contribution. (b),(c) The gluon-quark exchange diagrams considered in the RGM.

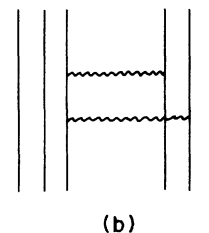
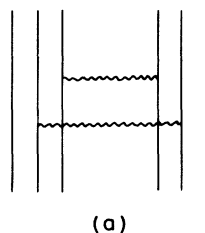


FIG. 2. (a),(b) Two-gluon exchange diagrams.

the Born approximation. Comparisons are to be made in the region where the Glauber approximation is applicable.

Formulas to estimate the contributions of two-gluon exchange diagrams to the NN spin-orbit t -matrix elements will be derived in Sec. II. Except for the use of Glauber theory, no further approximations will be made in the derivations. Numerical results, with comparisons to those calculated in the RGM,² will be presented in Sec. III for three different nucleon size parameters. Finally, a brief discussion about the results will be given in Sec. IV.

$$f^{(n)}(b) = \frac{(-1)^n}{n!} \sum'_{i_1, \dots, i_n=1}^3 \sum'_{j_1, \dots, j_n=1}^3 \left\langle \psi_i \psi_j \left| \prod_{m=1}^n \Gamma_{i_m j_m}(\mathbf{b} - \mathbf{S}_{i_m} + \mathbf{S}_{j_m}) \right| \psi_i(123) \psi_j(456) \right\rangle, \quad (2.2)$$

where primes indicate that the summations never run over the same (i_n, j_n) pair repeatedly, and \mathbf{k}_N and \mathbf{q} are, respectively, the incident nucleon's momentum and the momentum transfer in the NN center of mass system, \mathbf{b} the impact parameter, and \mathbf{S}_{i_m} the transverse component of the quark's position vector. The quark-quark scattering profile function, Γ , is related to the quark-quark scattering amplitude as

$$\Gamma_{lm}(b) = \frac{1}{2\pi i k} \int d^2 q e^{-i\mathbf{q} \cdot \mathbf{b}} F_{lm}(q), \quad (2.3)$$

k being the quark's relative momentum. The nucleon's wave function ψ_i is composed of three parts, namely

$$\psi_i = \phi_R(\text{spatial}) \phi_\sigma(\text{spin-isospin}) \phi_c(\text{color}), \quad (2.4)$$

with the spatial part being

$$\phi_R = (3\lambda^2/\pi^2)^{3/4} \exp \left\{ -\frac{\lambda}{2} [(\mathbf{r}_1 - \mathbf{r}_2)^2 + (\mathbf{r}_2 - \mathbf{r}_3)^2 + (\mathbf{r}_3 - \mathbf{r}_1)^2] \right\}, \quad (2.5)$$

where λ can be determined from nucleon's radius.

Through the transformation of

$$f^{(n)}(q) = \int d^2 b e^{i\mathbf{q} \cdot \mathbf{b}} f^{(n)}(b), \quad (2.6)$$

Eq. (2.1) then yields

$$F_{NN}(q) = \frac{ik_N}{2\pi} \left[- \sum_{n=1}^9 f^{(n)}(q) \right], \quad (2.7)$$

where the second-order term, $f^{(2)}(q)$, which contains two different kinds of two-gluon exchange diagrams, as shown in Fig. 2, is the main interest of the present work. After some manipulations, interaction amplitudes for these diagrams can be expressed as

$$f_1^{(2)}(q) = -18 \int d^2 q_1 d^2 q_2 \left\langle \frac{F_{14}(\mathbf{q}_1)}{k} \frac{F_{25}(\mathbf{q}_2)}{k} \right\rangle_{\lambda, \sigma} \times \delta(\mathbf{q} - \mathbf{q}_1 - \mathbf{q}_2) [g_2(q_1, q_2)]^2, \quad (2.8)$$

$$f_2^{(2)}(q) = -18 g_1(\mathbf{q}) \int d^2 q_1 d^2 q_2 \left\langle \frac{F_{14}(\mathbf{q}_1)}{k} \frac{F_{15}(\mathbf{q}_2)}{k} \right\rangle_{\lambda, \sigma} \times \delta(\mathbf{q} - \mathbf{q}_1 - \mathbf{q}_2) g_2(q_1, q_2), \quad (2.9)$$

II. TWO-GLUON EXCHANGE NN SPIN-ORBIT INTERACTION IN THE GLAUBER APPROXIMATION

In terms of quark-quark interactions, the NN scattering amplitude in the Glauber approximation⁴ is given by

$$F_{NN}(q) = \frac{ik_N}{2\pi} \int d^2 b e^{i\mathbf{q} \cdot \mathbf{b}} \left[- \sum_{n=1}^9 f^{(n)}(b) \right], \quad (2.1)$$

with

with the expectation values being taken over the color and the spin-isospin spaces, and $f_1^{(2)}(q)$ representing the sum of interactions similar to the diagram shown in Fig. 2(a), while $f_2^{(2)}(q)$ represents that of those similar to the diagram in Fig. 2(b). Of course,

$$f^{(2)}(q) = f_1^{(2)}(q) + f_2^{(2)}(q). \quad (2.10)$$

The form factors $g_1(q)$ and $g_2(\mathbf{q}_1, \mathbf{q}_2)$ in Eqs. (2.8) and (2.9) are defined as

$$g_m(\mathbf{q}_1, \dots, \mathbf{q}_m) = \int \exp \left[- \sum_{l=1}^m i\mathbf{q}_l \cdot \mathbf{r}_l \right] |\phi_R(\{\mathbf{r}_i\})|^2 \times \delta \left[\frac{\mathbf{r}_1 + \mathbf{r}_2 + \mathbf{r}_3}{3} \right] \prod_{j=1}^3 d^3 r_j \quad (2.11)$$

for $m \leq 3$. Use of the wave function of Eq. (2.5) therefore leads to

$$g_1(q) = \exp(-q^2/18\lambda), \quad (2.12)$$

$$g_2(\mathbf{q}_1, \mathbf{q}_2) = \exp[-(q_1^2 - \mathbf{q}_1 \cdot \mathbf{q}_2 + q_2^2)/18\lambda].$$

In order to keep the calculations simple, let us switch off all the other potentials and keep only the spin-orbit one. The quark-quark spin-orbit potential, as used in Ref. 2, is of the form

$$v_{mn}^{LS} = \lambda_m \cdot \lambda_n f(r_{mn})(\mathbf{r}_{mn} \times \mathbf{p}_{mn}) \cdot (\mathbf{s}_m + \mathbf{s}_n), \quad (2.13)$$

where λ is the eight-component color SU(3) generator, and the radial part $f(r)$, for the sake of simplicity and to enable it to be treated analytically, is chosen to be a Gaussian form of

$$f(r) = V_0 e^{-\mu r^2}, \quad (2.14)$$

μ being determined from the mean square radius of interaction and V_0 from the spin-orbit splittings of p -wave mesons, and chosen to be²

$$\mu = 1.5\lambda, \quad (2.15)$$

$$V_0 = -17.25[1 + \mu/(0.72 \text{ fm}^{-2})]^{2.5} \text{ MeV}.$$

To work out $f_1^{(2)}(q)$ and $f_2^{(2)}(q)$ in Eqs. (2.8) and (2.9), we first transform v_{mn}^{LS} into q space via the eikonal approximation, and obtain

$$F_{mn}(q) = \frac{k}{2\pi i} \int e^{iq \cdot b} \left\{ \exp \left[-\frac{iV_0}{\hbar v} \left(\frac{\pi}{\mu} \right)^{1/2} e^{-\mu b^2} \lambda_m \cdot \lambda_n \mathbf{b} \times \mathbf{k} \cdot (\mathbf{s}_m + \mathbf{s}_n) \right] - 1 \right\} d^2 b . \quad (2.16)$$

Inserting this together with Eq. (2.12) into Eq. (2.8), and performing q_i integrations, one obtains

$$f_1^{(2)}(q) = \frac{27\lambda}{2\pi} \exp(-q^2/36\lambda) \int d^2 b_1 d^2 b_2 \exp[-3\lambda(\mathbf{b}_1 - \mathbf{b}_2)^2/4] \exp \left[\frac{i\mathbf{q}}{2} \cdot (\mathbf{b}_1 + \mathbf{b}_2) \right] E_{1425}(\mathbf{b}_1, \mathbf{b}_2) , \quad (2.17)$$

with

$$E_{1425}(b_1, b_2) = \langle \{ \exp[se^{-\mu b^2} \lambda_1 \cdot \lambda_4 \mathbf{b}_1 \times \mathbf{k} \cdot (\mathbf{s}_1 + \mathbf{s}_4)] - 1 \} \{ \exp[se^{-\mu b^2} \lambda_2 \cdot \lambda_5 \mathbf{b}_2 \times \mathbf{k} \cdot (\mathbf{s}_2 + \mathbf{s}_5)] - 1 \} \rangle_{\lambda, \sigma} \quad (2.18)$$

and

$$s = -\frac{iV_0}{\hbar v} (\pi/\mu)^{1/2} . \quad (2.19)$$

$E_{1425}(\mathbf{b}_1, \mathbf{b}_2)$ can be expanded further in a power series,

$$E_{1425}(\mathbf{b}_1, \mathbf{b}_2) = \sum_{m=1}^{\infty} \sum_{n=1}^{\infty} \frac{s^{m+n}}{m!n!} C_{1425}(m, n) \times S_{1425}(m, n; \mathbf{b}_1, \mathbf{b}_2) e^{-\mu(m b_1^2 + n b_2^2)} , \quad (2.20)$$

with

$$S_{1425}(m, n; \mathbf{b}_1, \mathbf{b}_2) = \langle [\mathbf{b}_1 \times \mathbf{k} \cdot (\mathbf{s}_1 + \mathbf{s}_4)]^m \times [\mathbf{b}_2 \times \mathbf{k} \cdot (\mathbf{s}_2 + \mathbf{s}_5)]^n \rangle_{\sigma} \quad (2.21)$$

and

$$C_{1425}(m, n) = \langle (\lambda_1 \cdot \lambda_4)^m (\lambda_2 \cdot \lambda_5)^n \rangle_{\lambda} . \quad (2.22)$$

Before evaluating C_{1425} , let us examine the eight-component color operator λ . Taking the usual matrix representation,⁵ the components of λ obey the following well-known relationship when operating on the same particle j :

$$\lambda_{jl} \lambda_{jm} = \frac{2}{3} \delta_{lm} + \sum_n (d_{lmn} + i f_{lmn}) \lambda_{jn} , \quad (2.23)$$

where the structure constants d_{lmn} and f_{lmn} are, respectively, symmetric and antisymmetric under interchange of any pair of indices. Using the explicit magnitudes of d_{lmn} and f_{lmn} , one can deduce the following useful identities:

$$\sum_{l,m} f_{lmn} f_{lmt} = 3 \delta_{nt} , \quad (2.24)$$

$$\sum_{l,m} d_{lmn} d_{lmt} = \frac{5}{3} \delta_{nt} , \quad (2.25)$$

and

$$\sum_{m,n} d_{mmn} \lambda_n = 0 , \quad (2.26)$$

which further give

$$(\lambda_i \cdot \lambda_j)^n = C_n + d_n \lambda_i \cdot \lambda_j , \quad (2.27)$$

with

$$C_n = \frac{32}{9} d_{n-1} , \quad (2.28)$$

$$d_n = \frac{32}{9} d_{n-2} - \frac{4}{3} d_{n-1} \quad \text{for } n \geq 2 .$$

Apparently, $C_0 = 1$, $d_0 = 0$ and $C_1 = 0$, $d_1 = 1$.

With the help of Eqs. (2.27) and (2.28), as well as the nucleon's color singlet property, Eq. (2.22) then becomes simply

$$C_{1425}(m, n) = C_m C_n + d_m d_n \langle \lambda_1 \cdot \lambda_4 \lambda_2 \cdot \lambda_5 \rangle_{\lambda} , \quad (2.29)$$

where the color matrix element can readily be worked out for two color-singlet clusters, and reads

$$\langle \lambda_1 \cdot \lambda_4 \lambda_2 \cdot \lambda_5 \rangle_{\lambda} = \frac{8}{9} . \quad (2.30)$$

Also, in the case of $f_2^{(2)}(q)$, one obtains

$$\langle \lambda_1 \cdot \lambda_4 \lambda_1 \cdot \lambda_5 \rangle_{\lambda} = -\frac{16}{9} . \quad (2.31)$$

Having evaluated the color part, we now proceed to work on the spin expectation value of Eq. (2.21). With the z axis along \mathbf{k} , Eq. (2.21) is expanded in a power series as

$$S_{1425}(m, n; \mathbf{b}_1, \mathbf{b}_2) = \sum_{j=0}^m \sum_{l=0}^n \frac{m!}{j!(m-j)!} \frac{n!}{l!(n-l)!} \left[\frac{k}{2} \right]^{m+n} \times \langle (b_{1y} \sigma_{1x} - b_{1x} \sigma_{1y})^j (b_{1y} \sigma_{4x} - b_{1x} \sigma_{4y})^{m-j} (b_{2y} \sigma_{2x} - b_{2x} \sigma_{2y})^l (b_{2y} \sigma_{5x} - b_{2x} \sigma_{5y})^{n-l} \rangle_{\sigma} . \quad (2.32)$$

The complexity of Eq. (2.32) can be reduced further through the useful fact that

$$(b_y \sigma_x - b_x \sigma_y)^j = \frac{1}{2} \{ [1 - (-1)^j] b^j \sigma_x - b^j \sigma_y + [1 + (-1)^j] b^j \} , \quad (2.33)$$

which can be verified by mathematical induction. After some algebraic steps, including the explicit use of the three-quark cluster's spin-isospin wave function, Eq. (2.32) then becomes

$$S_{1425}(m, n; \mathbf{b}_1, \mathbf{b}_2) = \frac{k^{m+n}}{16} \{ [1 + (-1)^m][1 + (-1)^n][b_1^m b_2^n + b_1^{m-2} b_2^{n-2} (\mathbf{b}_1 \cdot \mathbf{b}_2)^2 / 9] \\ - 2[1 - (-1)^m][1 - (-1)^n]b_1^{m-1} b_2^{n-1} (\mathbf{b}_1 \cdot \mathbf{b}_2) / 3 \} , \quad (2.34)$$

which is nonzero only when integers m and n are both even or both odd. Thus starting from s^2 , $E_{1425}(\mathbf{b}_1 \cdot \mathbf{b}_2)$ in Eq. (2.20) includes only even powers of s . Inserting Eqs. (2.20), (2.29), (2.30), and (2.34) back into Eq. (2.17), one is then able to obtain the analytic form for $f_1^{(2)}(q)$ to any order of s , although this is tedious and time consuming.

$f_2^{(2)}(q)$ is calculated similarly and is given by

$$f_2^{(2)}(q) = \frac{27\lambda}{\pi} \exp(-5q^2/72\lambda) \int d^2b_1 d^2b_2 \exp[-3\lambda(\mathbf{b}_1 - \mathbf{b}_2)^2/2] \exp\left[\frac{i\mathbf{q} \cdot (\mathbf{b}_1 + \mathbf{b}_2)}{2}\right] E_{1415}(\mathbf{b}_1, \mathbf{b}_2) , \quad (2.35)$$

with

$$E_{1415}(\mathbf{b}_1, \mathbf{b}_2) = \sum_{m=1}^{\infty} \sum_{n=1}^{\infty} \frac{s^{m+n}}{m!n!} (C_m C_n - \frac{16}{9} d_m d_n) S_{1415}(m, n; \mathbf{b}_1, \mathbf{b}_2) e^{-\mu(mb_1^2 + nb_2^2)} \quad (2.36)$$

and

$$S_{1415}(m, n; \mathbf{b}_1, \mathbf{b}_2) = \frac{k^{m+n}}{16} \{ [1 + (-1)^m][1 + (-1)^n][b_1^m b_2^n - b_1^{m-2} b_2^{n-2} (\mathbf{b}_1 \cdot \mathbf{b}_2)^2 / 3] \\ + 2[1 - (-1)^m][1 - (-1)^n]b_1^{m-1} b_2^{n-1} (\mathbf{b}_1 \cdot \mathbf{b}_2) / 3 \} . \quad (2.37)$$

This completes the derivation of formulas for the two-gluon exchange contributions to the NN spin-orbit t -matrix element, which differs from the scattering amplitude $F_{NN}(q)$ of Eq. (2.7) by only a simple constant factor.

III. NUMERICAL RESULTS

Since $f^{(2)}(q)$ contains only even powers of s , the t -matrix element so calculated is purely imaginary. Curves denoted by $t^{(2)}$ in Figs. 3–7 are actually the t -matrix elements divided by i .

Calculations are done at $E_{\text{lab}} = 800$ MeV, with all the parameters being the same as those used in Ref. 2. Three sets of size parameter— $\lambda = \lambda_0$, $2\lambda_0$, and $4\lambda_0$ —are used with $\lambda_0 = \frac{1}{3}r_p^2 = 0.484 \text{ fm}^{-2}$, and are taken to fit the proton's radius at $r_p = 0.83 \text{ fm}$.

To avoid using the quark's momentum k and velocity v explicitly, one notes that s of Eq. (2.19) is inversely proportional to v , while s and k are in the same power throughout the calculations, as can be seen from Eqs. (2.20), (2.34), (2.36), and (2.37). One thus has

$$sk = -\frac{im_q V_0}{\hbar^2} (\pi/\mu)^{1/2} , \quad (3.1)$$

with $m_q = 0.17 \text{ GeV}$, the reduced quark mass.

Shown in Fig. 3 are contributions from $f_1^{(2)}(q)$, $f_2^{(2)}(q)$, and their sum for the case of $\lambda = \lambda_0$. We see that $t_1^{(2)}(q)$ and $t_2^{(2)}(q)$ display quite different characteristics. While the former stays positive and varies slowly through the calculated region, the latter increases from a negative value with a much sharper slope and becomes positive at around $q = 1.7 \text{ fm}^{-1}$. At the energy under consideration,

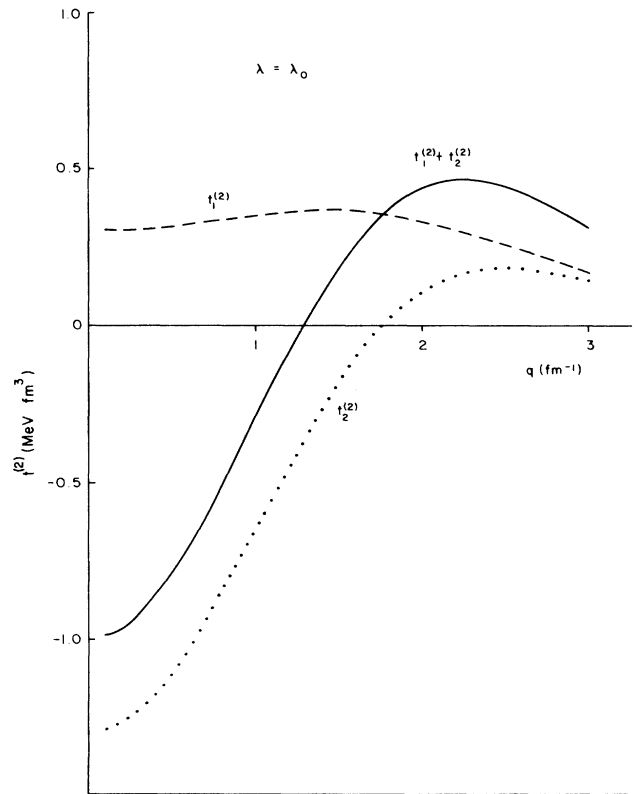


FIG. 3. T -matrix elements calculated from diagrams in Fig. 2 at $E_{\text{lab}} = 800$ MeV and $\lambda = \lambda_0$.

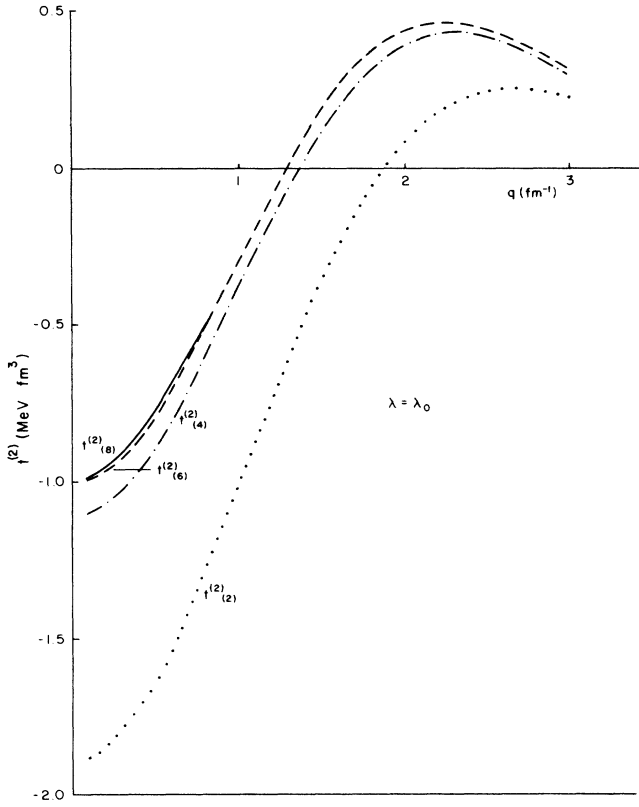


FIG. 4. Convergence test with $t^{(2)}(N)$ indicating that calculation is done up to the N th power of s .

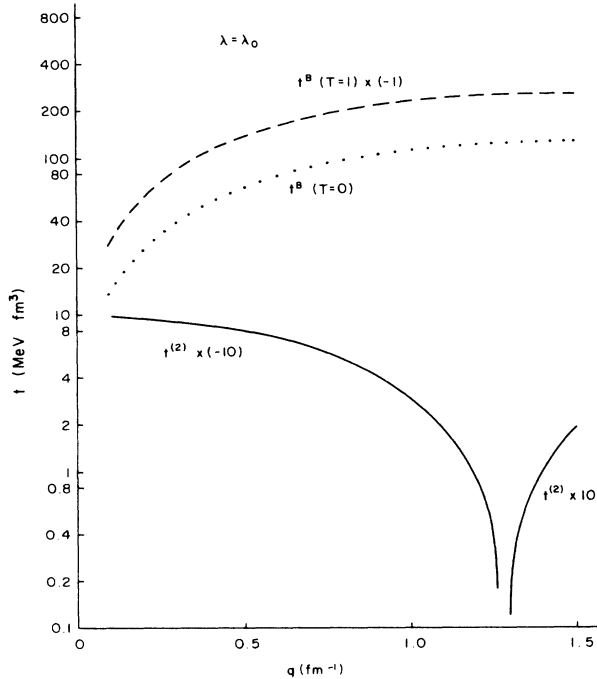


FIG. 5. Comparison for contributions from two-gluon exchange diagrams and from the RGM results in Ref. 2 at $E_{\text{lab}} = 800$ MeV and $\lambda = \lambda_0$.

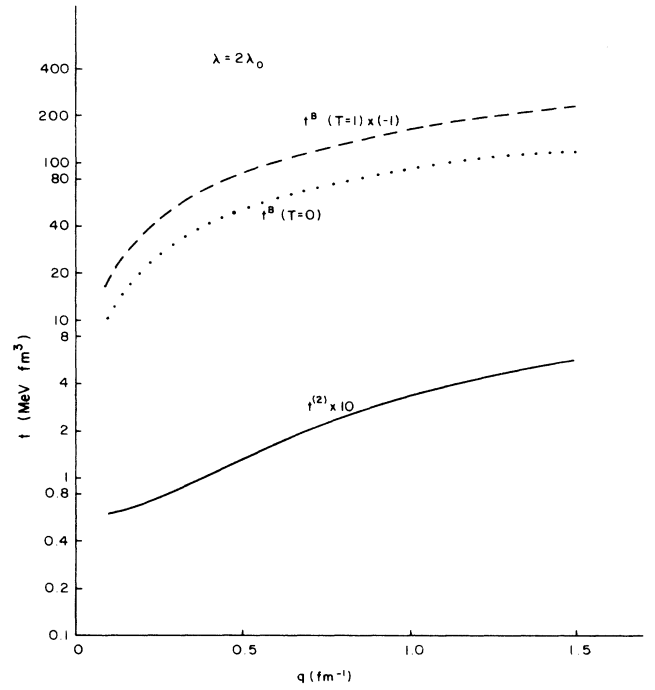


FIG. 6. Same as Fig. 5, except $\lambda = 2\lambda_0$.

the Glauber approximation may not give accurate results for $q \geq 2 \text{ fm}^{-1}$. The curves go beyond this only to show the characteristics of the series expansions for $f_1^{(2)}(q)$ in Eq. (2.17) and $f_2^{(2)}(q)$ in Eq. (2.35).

Calculations have been done up to s^{10} in the power series expansions of Eqs. (2.20) and (2.36). Convergence of these series are satisfactory. In Fig. 4, $t^{(2)}(N)$ denotes that calculation is done up to s^N . For the case of $\lambda = \lambda_0$, convergence is already reached at $N = 6$, while for cases of

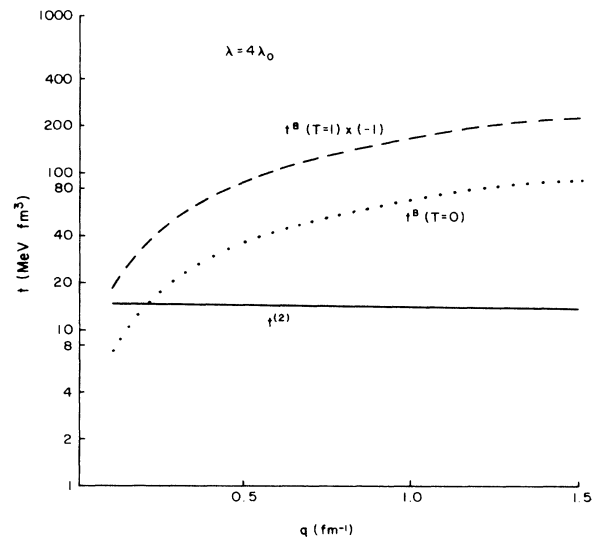


FIG. 7. Same as Fig. 5, except $\lambda = 4\lambda_0$.

larger λ , higher N may be required for convergence. In both of the other two cases, $N=10$ is adequate.

Since no isospin operator and no quark exchange are involved in the two-gluon exchange diagrams, the results of this work should be isospin independent. Hence the results are compared with both the $T=0$ and the 1 t -matrix elements calculated from the RGM,² denoted by t^B in Figs. 5–7 up to momentum transfer $q=1.5 \text{ fm}^{-1}$, where the Glauber approximation should be applicable for the energy currently considered.

In Fig. 5, comparisons are made for the $\lambda=\lambda_0$ case. As in Figs. 3 and 4, $t^{(2)}$ changes sign at around $q=1.25 \text{ fm}^{-1}$. The absolute value of $t^{(2)}$ starts at about one order of magnitude smaller than t^B , and then drops to more than two orders of magnitude smaller.

For the $\lambda=2\lambda_0$ case, although the magnitudes of $t_1^{(2)}(q)$ are greater than those in the $\lambda=\lambda_0$ case, strong cancellation occurs between $t_1^{(2)}(q)$ and $t_2^{(2)}(q)$ because, for most of the time, they have close absolute magnitudes, but with opposite signs. The resulting sum $t^{(2)}(q)$ is thus two orders of magnitude smaller than t^B , as seen from Fig. 6. In this case, the sign of $t^{(2)}(q)$ does not change.

For the $\lambda=4\lambda_0$ case, $t_2^{(2)}(q)$ becomes positive and about one order of magnitude smaller than $t_1^{(2)}(q)$. In the region of $q=0.1-1.5 \text{ fm}^{-1}$, $t_1^{(2)}(q)$ decreases slightly, while $t_2^{(2)}(q)$ increases slightly. As a result, their sum $t^{(2)}(q)$ drops only a few percent in this region. Another important fact shown in Fig. 7 is that this $t^{(2)}(q)$ can no longer be ignored when compared to t^B .

Calculations have also been done at $E_{\text{lab}}=425 \text{ MeV}$. The above general trends of $t^{(2)}(q)$ at $E_{\text{lab}}=800 \text{ MeV}$ are also preserved at this lower energy.

IV. CONCLUDING REMARKS

Although this work has been performed with the Gaussian radial function for the quark-quark spin-orbit interaction, results will most likely be similar when a

Breit-Fermi radial function is chosen. Wang and Wong² have shown that these two types of interactions give similar shapes and close magnitudes for the NN spin-orbit t -matrix elements in their RGM calculations.

The negligible contributions of the two-gluon exchange diagrams of the NN spin-orbit interaction at $\lambda=\lambda_0$ and $2\lambda_0$ confirm that the gluon-quark exchange diagrams considered in the RGM are indeed the lowest order ones, provided that the interaction range and the nuclear radius are not taken too small.

There could be several reasons for the non-negligible magnitudes of $t^{(2)}(q)$ at $\lambda=4\lambda_0$. First, one may question the validity of the Glauber approximation at this short interaction range. According to Eq. (2.25), the strength of the quark-quark spin-orbit interaction takes the value of $V_0=-980.46 \text{ MeV}$ at $\lambda=4\lambda_0$, 10 times as large as that at $\lambda=\lambda_0$. This may cause trouble for the Glauber approximation, which demands that $|V/(k^2/2m_q)|$ be much less than 1. On the other hand, for such a strong interaction it is also likely that the two-gluon exchange contributions cannot be ignored. Should this be the case, other multiple scattering terms in Eq. (2.1) may have to be included. In any case, results obtained from the RGM calculations might need to be modified should one treat the nucleon with this kind of small size. Possible meson-quark couplings and other relativistic effects might also have to be taken into account.

ACKNOWLEDGMENTS

This work was supported in part by the National Science Council of the Republic of China under Grant NSC76-0208-M001-33. It was completed during the author's visit to the National Research Institute for Mathematical Sciences of the Council for Scientific and Industrial Research (CSIR), Republic of South Africa. The author would like to thank the Institute's Theoretical Physics Division, headed by Dr. H. G. Miller, for their warm hospitality.

*Permanent address: Institute of Physics, Academia Sinica, Nankang Taipei, Taiwan 11529, Republic of China.

¹For examples, M. B. Kislinger, Phys. Lett. **79B**, 474 (1978); H. J. Pirner, *ibid.* **85B**, 190 (1979); C. S. Warke and R. Shanker, Phys. Rev. C **21**, 2643 (1980); O. Morimatsu, S. Ohta, K. Shimizu, and K. Yazaki, Nucl. Phys. **A420**, 573 (1984); Y. Suzuki and K. T. Hecht, *ibid.* **A420**, 525 (1984); O. Morimatsu and K. Yazaki, *ibid.* **A424**, 412 (1984); K. Holinde, Phys. Lett. **157B**, 123 (1985).

²Fan Wang and Chun Wa Wong, Nucl. Phys. **A438**, 620 (1985).

³J. A. Wheeler, Phys. Rev. **52**, 1083 (1937); C. W. Wong, Phys. Rep. **15c**, 283 (1975).

⁴R. J. Glauber, in *Lectures in Theoretical Physics*, edited by W. E. Britten and L. G. Dunham (Interscience, New York, 1959), Vol. I, p. 315.

⁵M. Gell-Mann, Phys. Rev. **125**, 1067 (1962).